PHYSICAL REVIEW A **85**, 035803 (2012)

# Photonic heterostructures with Lévy-type disorder: Statistics of coherent transmission

A. A. Fernández-Marín and J. A. Méndez-Bermúdez
*Instituto de Física, Benemérita Universidad Autónoma de Puebla, Apartado Postal J-48, Puebla 72570, Mexico*

Victor A. Gopar
*Departamento de Física Teórica, Facultad de Ciencias, and Instituto de Biocomputación y Física de Sistemas Complejos, Universidad de Zaragoza, Pedro Cerbuna 12, E-50009 Zaragoza, Spain*
(Received 16 January 2012; published 26 March 2012)

We study the electromagnetic transmission $T$ through one-dimensional (1D) photonic heterostructures whose random layer thicknesses follow a long-tailed Lévy-type distribution. Based on recent predictions made for 1D coherent transport with Lévy-type disorder, we show numerically that for a system of length $L$ (i) the average $\langle -\ln T\rangle \propto L^\alpha$ for $0 < \alpha < 1$, while $\langle -\ln T\rangle \propto L$ for $1 \leqslant \alpha < 2$, $\alpha$ being the exponent of the power-law decay of the layer-thickness probability distribution, and (ii) the transmission distribution $P(T)$ is independent of the angle of incidence and the frequency of the electromagnetic wave, but it is fully determined by the values of $\alpha$ and $\langle \ln T\rangle$. Additionally we have found and numerically verified that $\langle T\rangle \propto L^{-\alpha}$ with $0 < \alpha < 1$.

DOI: 10.1103/PhysRevA.85.035803 PACS number(s): 42.25.Dd, 03.65.Nk, 72.15.Rn

Random processes characterized by density probabilities with a long tail (Lévy-type processes) have been found and studied in very different phenomena and fields such as biology, economy, and physics. One of the main features of a Lévy-type density distribution, $p(l)$, is the slow decay of its tail. More precisely, for large $l$,

$$p(l) \sim \frac{1}{l^{1+\alpha}}, \tag{1}$$

with $0 < \alpha < 2$. Note that the second moment diverges for all $\alpha$ and if $0 < \alpha < 1$ also the first moment diverges. These kind of distributions are also known as $\alpha$-stable distributions [1]. A window on new optical materials which allow for the experimental study of Lévy flights in an outstanding controllable way was recently opened with the construction of the so-called *Lévy glass* [2]: titanium dioxide particles are suspended in a matrix made of glass microspheres. The distribution of the microsphere diameters is properly chosen in order that light can travel by performing Lévy flights within the microspheres. The diameter distribution is characterized by the exponent $\alpha$ of the power-law decay of its tail; it was found [2] that when $0 < \alpha < 1$ the transport is superdiffusive, while for $\alpha = 2$ the normal diffusive transport is recovered. This experimental investigation has motivated several theoretical works on the effects of the presence of Lévy-type processes on different transport quantities in one dimension, as well as in higher dimensional systems [3–7].

On the other hand, coherent electron transport through one-dimensional (1D) quantum wires with Lévy-type disorder was studied in Ref. [6]. It was found that for the dimensionless conductance, or transmission, $T$,

(i) the average (over different disorder realizations) of the logarithm of the transmission behaves as

$$\langle -\ln T\rangle \propto \begin{cases} L^\alpha & \text{for} \quad 0 < \alpha < 1, \\ L & \text{for} \quad 1 \leqslant \alpha < 2, \end{cases} \tag{2}$$

and

(ii) the distribution of transmission $P(T)$ is fully determined by the exponent $\alpha$ and the ensemble average $\langle \ln T\rangle$.

We point out that although for $1 \leqslant \alpha < 2$, the average $\langle \ln T\rangle$ depends linearly on $L$, as in the standard Anderson localization problem, it is interesting to remark that the statistical properties of $T$ are not those predicted by the standard scaling approach to localization, in particular by the Dorokhov-Mello-Pereyra-Kumar (DMPK) equation [8]. That is, for $1 \leqslant \alpha < 2$ the transmission fluctuations are larger than those considered in the DMPK equation. Thus, the standard statistical properties of $T$ are recovered for $\alpha \geqslant 2$.

Having as a reference various analogies between electron, light, and matter-wave transport [9–13] one may expect the statements (i) and (ii) to be also valid for 1D optical systems, even though in the latter case additional parameters such as incidence angle and frequency come into play. A systematic investigation of the statistical properties of coherent transmission for a 1D analog of Lévy glasses is not available in the literature and the above expectations have not been verified until now. Therefore, in this paper we undertake this task by studying the transmission $T$ through 1D photonic heterostructures with Lévy-type spacing disorder. Moreover, engineering the disorder in a photonic heterostructure might be a less complex task than in an electronic system; so we hope that this work stimulates future photonic experiments.

The heterostructures that we shall study consist of an alternating sequence of layers of materials $A$ and $B$ having refractive indexes $n_A$ and $n_B$, respectively. See Fig. 1. The corresponding thicknesses $l_A$ and $l_B$ are chosen as random numbers drawn from a Lévy-type distribution characterized by the exponent $\alpha$ of its power-law tail. In this work we only consider Lévy-type distributions supported along the positive semiaxis and focus on the case $0 < \alpha < 1$, where large fluctuations of the transmission produce the most interesting effects. The total length $L$ of the heterostructure is then given by $L = \sum l_j$. Without loss of generality we consider that the heterostructure grows in the $z$ direction.

One-dimensional heterostructures with Lévy-type thickness disorder, as defined above, can be produced with porous silicon. Layers of silicon with different porosities (i.e., different refractive indexes) and varying thicknesses can be obtained

 

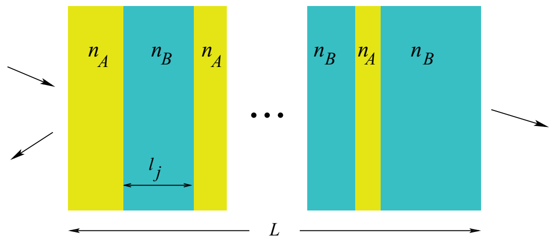


FIG. 1. (Color online) Sketch of a heterostructure of length $L$ with random layer thicknesses $l_j$ and refractive indexes $n_{A(B)}$. The distribution of the thicknesses follows a Lévy-type distribution.

by fluorhydric acid electrochemical etching by modulating the value of the current density during the anodization process [14]. Thus we fix $n_A = 1.4$ and $n_B = 2.4$ in our calculations since they correspond to experimentally accessible porous silicon refractive index values [14,15].

We compute the transmission $T$ through our 1D heterostructure using the transfer matrix formalism described in Ref. [16]. We consider an electromagnetic wave with frequency $\omega$ that strikes the first layer of the heterostructure (embedded in air) making an angle $\theta$ with respect to the $z$ axis, then propagates inside the structure composed of $N$ layers, and finally escapes through the layer on the opposite side. Without loss of generality, in the following we specialize on TE modes. The transfer matrix of the scattering process can be written as [16]

$$\mathbf{M} = \mathbf{M}_{0,N}\mathbf{M}_{\text{het}}\mathbf{M}_{1,0}, \tag{3}$$

where $\mathbf{M}_{\text{het}} = \mathbf{D}_N\mathbf{M}_{N,N-1}\mathbf{D}_{N-1}\cdots\mathbf{M}_{2,1}\mathbf{D}_1$,

$$\mathbf{D}_j = \begin{pmatrix} \exp(ik_{jz}l_j) & 0 \\ 0 & \exp(-ik_{jz}l_j) \end{pmatrix},$$

$$\mathbf{M}_{j,j-1} = \frac{1}{2}\begin{pmatrix} 1 + k_{(j-1)z}/k_{jz} & 1 - k_{(j-1)z}/k_{jz} \\ 1 - k_{(j-1)z}/k_{jz} & 1 + k_{(j-1)z}/k_{jz} \end{pmatrix},$$

and $k_{jz}$ is the component of the wave vector along the $z$ direction in the $j$th layer given by $k_{jz} = k_j\cos(\theta_j)$, with $k_j = (\omega/c)n_j$ ($n_j$ equals $n_A$ or $n_B$). $\theta_j$ is related to $\theta_{j-1}$ through Snell's law: $\sin(\theta_j)/\sin(\theta_{j-1}) = n_{j-1}/n_j$. Above, $\mathbf{M}_{1,0}$ [$\mathbf{M}_{0,N}$] is the transfer matrix for the interface between the first [$N$th] layer and air, while $\mathbf{M}_{\text{het}}$ is the transfer matrix of the heterostructure. Finally,

$$T = |\mathbf{M}_{22}|^{-2}. \tag{4}$$

In the following we study the statistical properties of $T$, in particular its full distribution. Concerning the numerical simulations along this work, the statistics is collected over an ensemble of different disorder realizations. Notice that since the thicknesses $l_i$ are drawn from a Lévy-type distribution, Eq. (1), for a fixed length $L$ the number of layers composing a heterostructure might vary strongly from sample to sample. Throughout the paper, $\omega$ is given in units of the reference frequency $\omega_0 = 2\pi c/\lambda_0$, where $\lambda_0$ could be chosen to provide suitable experimental conditions.

As we have mentioned, the theoretical results in this paper are based on the analysis presented in Ref. [6]. Here we only

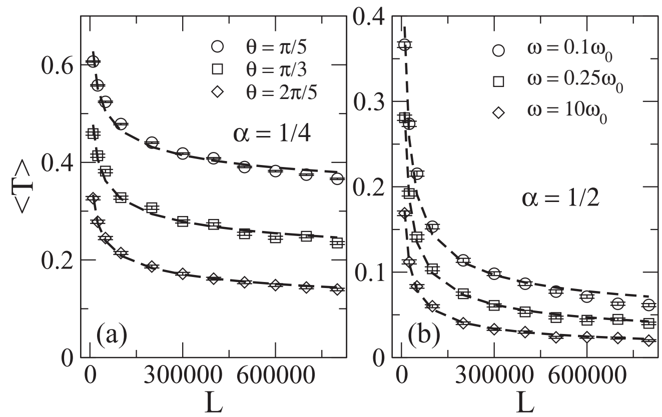


FIG. 2. Average transmission $\langle T\rangle$ as a function of $L$ (symbols) for 1D heterostructures with Lévy-type spacing disorder characterized by $\alpha$. In panel (a) [(b)] three values of $\theta$ [$\omega$] were considered for $\omega = 0.25$ [$\theta = 0$]. Dashed curves are fittings of the numerical data accordingly to Eq. (7). Each symbol was calculated using $10^4$ ensemble realizations.

reproduce the main result of that work: the distribution for transmission $P_\xi(T)$ with $\xi \equiv \langle \ln T\rangle$. The average quantities that we study, such as $\langle T\rangle$ and $\langle \ln T\rangle$ [Eq. (2)], are derived from the following expression for the distribution:

$$P_\xi(T) = \int_0^\infty p_{s(\alpha,\xi,x)}(T)q_{\alpha,1}(x)dx, \tag{5}$$

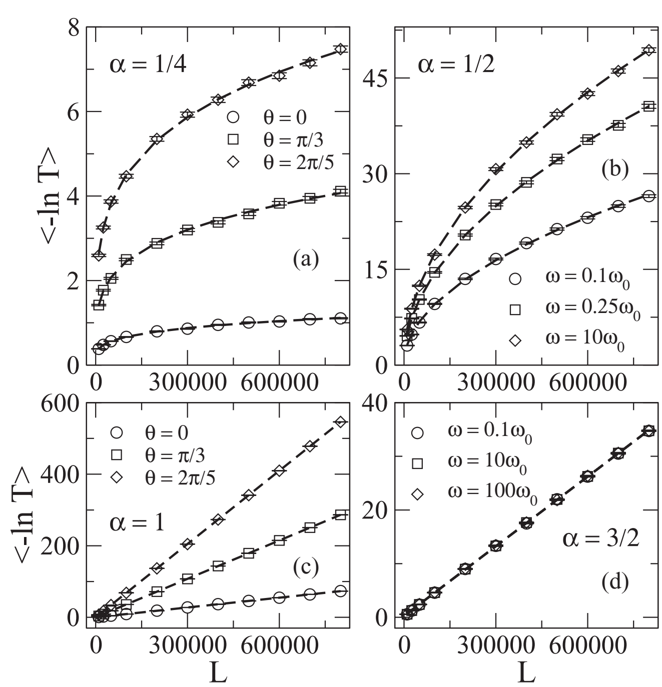


FIG. 3. The average $\langle -\ln T\rangle$ as a function of $L$ (symbols) for 1D heterostructures with Lévy-type spacing disorder characterized by $\alpha$. In panels (a) and (c) [(b) and (d)] three values of $\theta$ [$\omega$] were considered for $\omega = 0.25$ [$\theta = 0$]. The dashed curves are fittings of the data with Eq. (2). Each symbol was calculated using $10^4$ ensemble realizations.

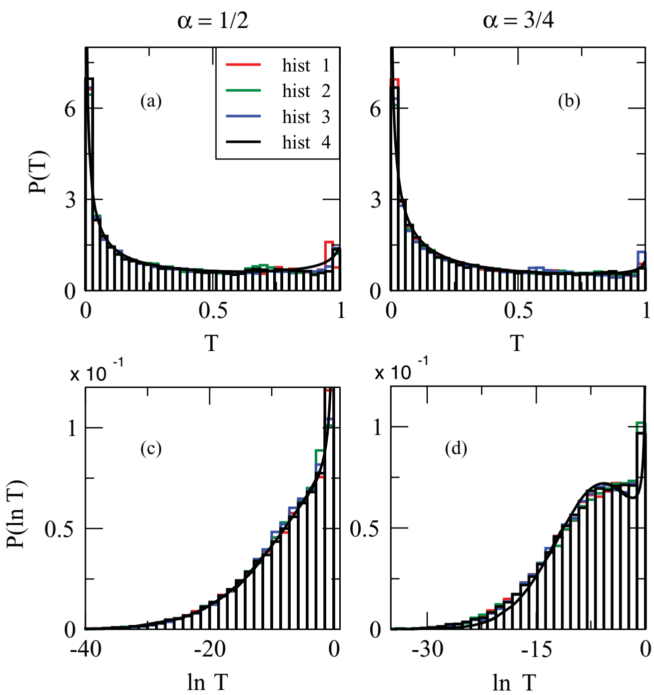


FIG. 4. (Color online) The probability distribution functions $P(T)$ [(a) and (b)] and $P(\ln T)$ [(c) and (d)] for $\alpha = 1/2$ and 3/4 (histograms). Each panel contains four histograms with values of $\theta$ and $\omega$ given in Table I. The histograms in panels (a) and (b) [(c) and (d)] are characterized by $\langle -\ln T\rangle \approx 2$ [$\langle -\ln T\rangle \approx 8$]. Black dashed curves are the corresponding theoretical predictions obtained from Eq. (5). Each histogram was calculated using $3 \times 10^4$ ensemble realizations.

for $0 < \alpha < 1$, where $q_{\alpha,c}$ is the probability density function of the Lévy-type distribution supported in the positive semiaxis, $s(\alpha,\xi,x) = \xi/(2x^\alpha I_\alpha)$, $I_\alpha = 1/2\int_0^\infty x^{-\alpha} q_{\alpha,1} dx$, and

$$p_s(T) = \frac{s^{-3/2}}{\sqrt{2\pi}} \frac{\exp(-s/4)}{T^2} \int_{y_0}^{\infty} dy \frac{y\ \exp(-y^2/4s)}{\sqrt{\cosh y + 1 - 2/T}}, \tag{6}$$

where $y_0 = \text{arcosh}(2/T - 1)$.

We start by analyzing the average transmission $\langle T\rangle$. From Eq. (5), we find that

$$\langle T\rangle \propto L^{-\alpha}, \tag{7}$$

for $0 < \alpha < 1$. We have verified numerically this result. In Fig. 2 we present the average transmission for different values of $\theta$ and $\omega$ for $\alpha = 1/4$ and $\alpha = 1/2$. As we can see, the agreement is very good in all cases. This result, Eq. (7), could be contrasted with the exponential decay of $\langle T\rangle$ with $L$, for standard 1D disordered systems, and with $\langle T\rangle \propto 1/L$, for quasi-1D systems in the normal diffusive transport regime.

We now study the average $\langle \ln T\rangle$. In electronic transport this quantity is of relevance since it gives information about the localization length of the disordered system. In Fig. 3 we present different plots of the average $\langle \ln T\rangle$ as a function of $L$ for $\alpha < 1$ [Figs. 3(a) and 3(b)] and $\alpha \geqslant 1$ [Figs. 3(c) and 3(d)]. For $\alpha < 1$ we observe a clear behavior of the form $\langle -\ln T\rangle \propto L^\alpha$; while for $\alpha \geqslant 1$ we see that $\langle -\ln T\rangle$ is simply proportional to $L$, as for standard 1D disordered systems. Therefore, all curves in Fig. 3 are well described by Eq. (2). In addition, notice that while the curves of $\langle \ln T\rangle$ vs $L$ strongly depend on the incidence angle $\theta$ for all $\alpha$ [see Figs. 3(a) and 3(c)], the dependence on $\omega$ is lost for $\alpha \geqslant 1$ [see Figs. 3(b) and 3(d)].

TABLE I. Values of $(\theta,\omega/\omega_0)$ used for the histograms in Fig. 4.

| Panel | hist 1 | hist 2 | hist 3 | hist 4 |
|---|---|---|---|---|
| (a) | (0,0.1) | $(\pi/5,0.5)$ | $(\pi/4,10)$ | $(3\pi/7,1)$ |
| (b) | (0,10) | $(\pi/5,1)$ | $(\pi/6,0.1)$ | $(\pi/3,0.5)$ |
| (c) | (0,10) | $(\pi/5,5)$ | $(2\pi/5,1)$ | $(\pi/6,0.1)$ |
| (d) | (0,2) | $(\pi/4,10)$ | $(\pi/5,1)$ | $(\pi/3,5)$ |

Next, we analyze the full distribution of the transmission. It is clear from Fig. 3 that by choosing the appropriate combination of $\theta$, $\omega$, and $L$ one can fix the value of the average $\langle \ln T\rangle$ for a given $\alpha$. Then, in Figs. 4(a) and 4(b) we show probability distribution functions $P(T)$ for $\alpha = 1/2$ and 3/4 for $\langle -\ln T\rangle \approx 2$. Since for smaller values of $\langle \ln T\rangle$, $P(T)$ is concentrated close to $T = 0$, in Figs. 4(c) and 4(d) we present $P(\ln T)$ for $\langle -\ln T\rangle \approx 8$. Notice that each panel in this figure contains four histograms with different combinations of $\theta$ and $\omega$. However, all histograms fall one on top of the other; that is, $P(T)$ and $P(\ln T)$ are completely determined by $\alpha$ and $\langle \ln T\rangle$. Moreover, the black lines are the corresponding theoretical predictions for $P(T)$ and $P(\ln T)$ for the specific combinations of $\alpha$ and $\langle \ln T\rangle$ we used. Evidently, the correspondence between theory and numerics is excellent, affirming the equivalence between quantum and electromagnetic 1D disordered systems.

Finally, we want to stress that even though we have used arbitrary units for the length $L$ of the heterostructures, our results may be experimentally confirmed by properly choosing the frequency $\omega = 2\pi c/\lambda$. For instance, since $\omega/\omega_0 = \lambda_0/\lambda$, if $\lambda_0 = 2L$ a typical experiment in the visible range with $\lambda \sim 500$ nm and $L \sim 10$ microns [14,15] will set the ratio $\omega/\omega_0$ to 40. Then, $\theta$ can be tuned to specify a desired value of $\langle T\rangle$ or $\langle \ln T\rangle$.

In summary, for 1D heterostructures whose layer thicknesses follow a Lévy-type distribution, characterized by a power-law decay, we have shown that $\langle -\ln T\rangle \propto L^\alpha$ for $0 < \alpha < 1$; and once $\alpha$ and $\langle \ln T\rangle$ are fixed the distribution of transmission $P(T)$ is invariant with respect to the system parameters $(\theta,\omega)$. Also, we have found that $\langle T\rangle \propto L^{-\alpha}$, in contrast to the exponential decay in standard disordered 1D systems. We have verified that our results are unaffected by considering TM modes and different refraction index contrasts $n_A/n_B$.

We hope that our results serve to deepen our understanding of transport properties when Lévy-type disorder is present and motivate further experimental investigation on its unconventional effects, such as those shown in this work.

This work was partially supported by VIEP-BUAP (Project MEBJ-EXC10-I), Mexico, and MICINN (Project FIS2009-07277), Spain.

[1] V. V. Uchaikin and V. M. Zolotarev, *Chance and Stability. Stable Distributions and Their Applications* (VSP, Utrecht, 1999).
[2] P. Barthelemy, J. Bertolotti, and D. S. Wiersma, Nature (London) **453**, 495 (2008).
[3] C. W. J. Beenakker, C. W. Groth, and A. R. Akhmerov, Phys. Rev. B **79**, 024204 (2009).
[4] R. Burioni, L. Caniparoli, and A. VezzaniPhys. Rev. E **81**, 060101(R) (2010).
[5] P. Buonsante, R. Burioni, and A. Vezzani, Phys. Rev. E **84**, 021105 (2011).
[6] F. Falceto and V. A. Gopar, Europhys. Lett. **92**, 57014 (2010).
[7] R. T. Sibatov, JETP Lett. **93**, 503 (2011).
[8] P. A. Mello and N. Kumar, *Quantum Transport in Mesoscopic Systems* (Oxford University Press, Oxford, 2004).
[9] B. A. van Tiggelen and A. Tip, J. Phys. I (Fr.) **1**, 1145 (1991).
[10] P. Sheng, *Introduction to Wave Scattering, Localization, and Mesoscopic Phenomena* (Academic Press, San Diego, 1995).
[11] G. L. J. A. Rikken and B. A. van Tiggelen, Nature (London) **381**, 54 (1996).
[12] R. Sapienza, P. Costantino, D. Wiersma, M. Ghulinyan, C. J. Oton, and L. Pavesi, Phys. Rev. Lett. **91**, 263902 (2003).
[13] F. Scheffold and G. Maret, Phys. Rev. Lett. **81**, 5800 (1998).
[14] A. Bruyant, G. Lerondel, P. J. Reece, and M. Gal, Appl. Phys. Lett. **82**, 3227 (2003).
[15] J. O. Estevez, J. Arriaga, A. M. Blas, and V. Agarwal, Appl. Phys. Lett. **93**, 191915 (2008).
[16] P. Markos and C. M. Soukoulis, *Wave Propagation: From Electrostatics to Photonic Crystals and Left-Handed Materials* (Princeton University Press, Princeton, NJ, 2008).